The effect of drying-wetting cycles on the seismic properties of an anisotropic claystone

G. Mitaritonna, J. Pineda, M. Arroyo & E. Romero
Department of Geotechnical Engineering, UPC, Barcelona, Spain

ABSTRACT

The evolution of bar and shear wave velocities during a drying wetting cycle on a claystone is presented. There is a clear relationship with total suction, established by means of the material water retention curve. The stiffening effect of drying decreases with sample damage. The multiaxial bender element technique is firstly applied to rock-like materials with partial success.

1. INTRODUCTION

Due to the specific characteristics of argillaceous soft rocks, such as low permeability, a self-healing capacity when fractured but also the significant retardation properties for solute transport, these materials are being considered as a potential host geological media for underground repositories of high-level radioactive waste around the world [1]. Several underground laboratories has been constructed to evaluate the response of this geological media under construction and operational conditions. Within this group lies the Mont Terri underground laboratory (Switzerland), excavated in Opalinus clay. Several in-situ tests have been performed on this clay, e.g., the heating (HE-D) test, [1]. The main physical and geotechnical parameters obtained from laboratory and in-situ tests can be found in [3]. Recent research [1,2] has proven that the Opalinus clay THM response is anisotropic. Mechanical anisotropy is visible, for instance, in elastic moduli. In materials like Opalinus clay, these elastic moduli will likely vary with porosity, degree of saturation and temperature.

In this paper some results of an experimental program on natural Opalinus clay are presented. The program investigated the influence of environmental actions, like wetting-drying cycles on the anisotropic stiffness of natural Opalinus clay. Shear ($V_{s(ij)}$, $G_{(ij)}$) and compression ($V_{l(i)}$, $E_{(i)}$) elastic parameters were measured using two non-destructive techniques: multiaxial bender elements [4] and a conventional ultrasonic pulse device. The multiaxial bender element technique had not been previously employed on very stiff materials like Opalinus clay. Thus, exploring its applicability to a stiff material was one aim of the present work.

Giuseppina Mitaritonna, Jubert Pineda, Marcos Arroyo and Enrique Romero, Department of Geotechnical Engineering and Geosciences, Universitat Politècnica de Catalunya, Jordi Girona 1-3, 08034Barcelona, Spain

2. CHARACTERISCTIC OF OPALINUS CLAY

2.1. Basic characterization and porosimetry

Opalinus clay is a stiff overconsolidated clay of Lower Aalenian age, corresponding to the Middle Jurassic. Contains between 40 to 80% clay minerals (illite, smectite, chlorite, kaolinite), carbonates (calcite, dolomite, ankerite and siderite) and quartz [5].
At Mont Terri overburden varies between 250m and 350m and closely spaced bedding dips at an angle of about 45º. Samples tested in this work were obtained from horizontal borehole BHE-D26, directed from a niche towards the heating test HE-D area. At this location a damaged zone, with lower stiffness and higher permeability, was identified by numerical backanalysis of the heating test [1]. Two samples, hereafter named S-1 and S-2 respectively, were taken at 0.2m and 0.5m from the heater. The basic properties of these samples are listed in Table 1 alongside average values for the clay [1, 6].

TABLE 1.MAIN PHYSICAL PROPERTIES OF OPALINUS CLAY

	ρ_d (Mg/m^3)	ρ_s (Mg/m^3)	w (%)	Total suction, Ψ (MPa)	n	Sr	w_L (%)	PI (%)
Average value	2.22-2.33¶	2.73± 0.01*	4.2 -8¶	10–16*	0.13–0.18¶	0.83–0.93*	-	-
Samples tested	2.28±0.01	2.73± 0.01	5.8 - 6.5	22-28	0.163	0.83	40.5	24

¶ data from [1] * data from [6]

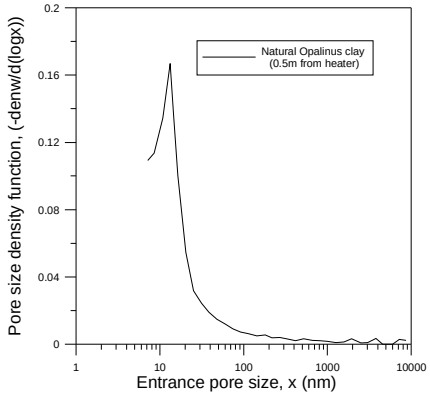

Figure 1. Pore size distribution of natural Opalinus clay S-2 specimen

Mercury intrusion porosimetry, Figure 1 was performed on a freeze-dried S-2 specimen. One dominant pore mode about 15 nm appears, as expected for the matrix type microstructure common in argillaceous rocks [6].

2.2. Water retention properties

The water retention curve (WRC) of S-2 specimen, expressed as total suction versus gravimetric water content, was obtained by means of a chilled-mirror dew-point psychrometer (WP4, [7]), during a wetting-drying-wetting cycle under unconfined conditions. An air drying procedure induced suction increase until a relative humidity (RH) of 50%, then a vapour equilibrium technique [8] using lithium chloride (LiCl) took RH to 15%. The wetting path was also imposed by vapour equilibrium, using distilled water to apply a RH around 99%.

Each suction measurement by means of WP4 was made after 24 hours to ensure specimen equalization. Calibration and test procedure followed Cardoso et al. [9]. Figure 2 shows the drying and wetting branches of the water retention curve. A small hysteretic loop is observed between drying and wetting paths for suction values between 4MPa and 120MPa. The variation in total suction obtained during a wetting-drying cycle ranged from 1MPa to 221MPa, for RH of 98% and 15%, respectively.

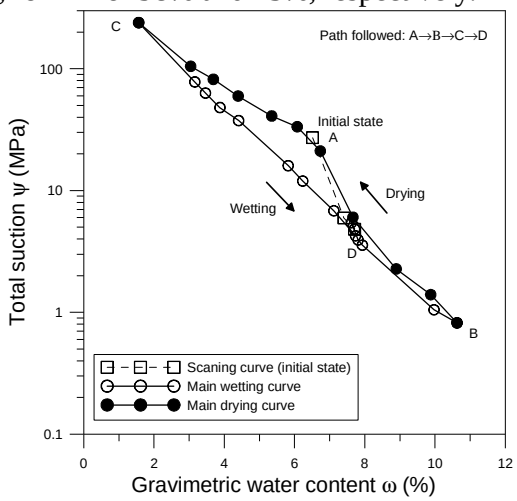

Figure 2. Water retention curve for Opalinus clay at 0.5m from heater

3. EXPERIMENTAL DETAILS

Only two specimens, S-1 and S-2, were obtained from the larger diameter cores using a drilling machine by air circulation. Specimen dimension was limited for (i) the borehole dimensions (90mm in diameter); and, (ii) manufacture procedure (complicated because of anisotropy and water sensitivity). Specimens were cut perpendicular to the borehole so that bedding planes had their natural dip angle (45º) (Figure 3a). In Table 2 the initial conditions for the specimens are listed:

TABLE 2.INITIAL CONDITIONS FOR SAMPLES TESTED

Sample	ϕ mm)	h(mm)	ω (%)	ρ (Mg/m3)	Ψ (MPa)	n	Sr
S-1	38	75	6.2	2.42	29	0.165	0.86
S-2	38	55	5.7	2.38	35	0.165	0.75

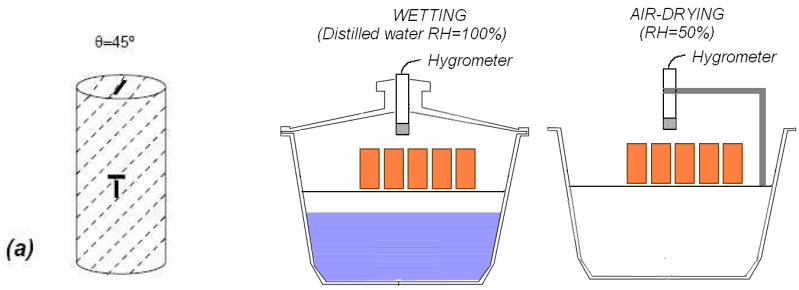

Figure 3. a) Specimen set up; b) Experimental set-up to perform a wetting-drying cycle

3.1. Wetting-drying cycle

One wetting-drying cycle was applied using the vapour equilibrium technique described in section 2.2. To simulate “in-situ” conditions at Mont Terri Laboratory, RH ranged

between 99% and 50%. Figure 3b shows the experimental set-up used in the test. Porosity and water content were tracked using volume and weight measurements.

3.2 Shear modulus measurements

Bender elements [10], were employed to measure multidirectional very small strain shear stiffness $G_{(ij)} = \rho_t V^2_{s(ij)}$, where ρ_t is the total density, $V_{s(ij)} = l_i/t_s$ is the velocity of the shear waves through the specimen and the first subscript denotes measurement direction and the second input polarization direction. The wave travel distance (l_i) is taken as the distance between transducer tips [11]. Arrival time (t_s) is determined by inspection of the received trace, looking for the first significant amplitude excursion.
Bender elements, measuring along the sample vertical axis, had been previously applied in rocks by Pineda et al. [13]. One step further was to employ horizontally mounted bender elements, like those in use for clays [4]. Two bender transducers, in a T-shaped configuration (Fig. 4a), were housed in a brass cup filled with resin. The transducer housings were then adhered to the specimen lateral surface at middle height. Vertically mounted transducers protrude about 4mm into pre-drilled slots on the sample and horizontal ones about 5mm; silicone grease is used for coupling.

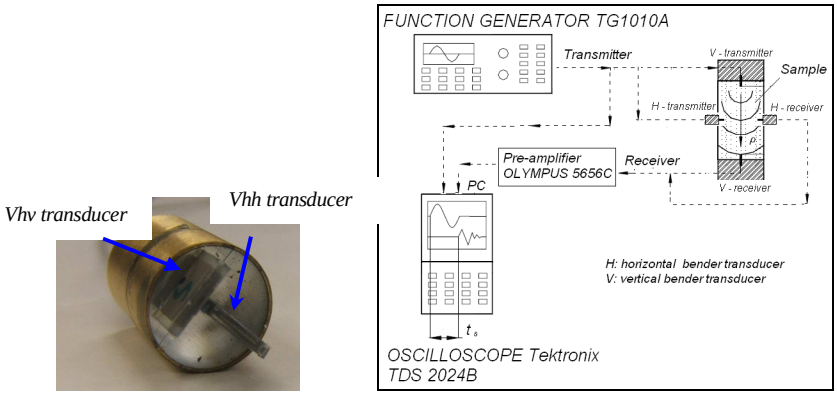

Figure 4. a) Horizontal T-shaped bender probe, b) Experimental set-up used during bender elements tests

The experimental set-up (Figure 4b), included a function generator (Thurlby Thandar® TTi -TG1010A), digital oscilloscope (Tektronix® TDS2024b) and amplifier (OLYMPUS® Panametrics 56456C). Input amplitude was fixed at ±10 V peak to peak.
For vertical measurements, a single sine pulse (apparent frequency = 50kHz) was used, and for the horizontal, a sine burst (apparent frequency = 12kHz). More details about the use of bender elements in rock-like materials, including their implementation on a newly developed triaxial cell may be found in Pineda [12].

3.3 Young modulus measurements

The bar wave velocity was measured using an ultrasonic pulse device (V-Meter®). This device is used to determine the travel time (t_p) of a higher frequency and voltage signal (f_{app}= 54kHz V_{input}=500V respectively). Young modulus was obtained from the bar wave ($E_{u(i)} = \rho_t V^2_{L(i)}$)

4. EXPERIMENTAL RESULTS

4.1 Hydraulic loading and volumetric behaviour

Figures 5a,b show, for both specimens, the wetting-drying path followed and the corresponding porosity evolution. The wetting path lead both specimens to a final water content of around 7.5%. Water adsorption rates (Fig. 5a) were similar in both specimens, reaching a constant mass state after five days. Drying proceeded at a somewhat slower pace, with specimens experiencing a quick initial drop in gravimetric water content and reaching a constant mass state after 13 days. The final gravimetric water content at the end of drying stage was around 2.6% corresponding to a total suction about 100MPa as indicated by the WRC (Fig. 2).

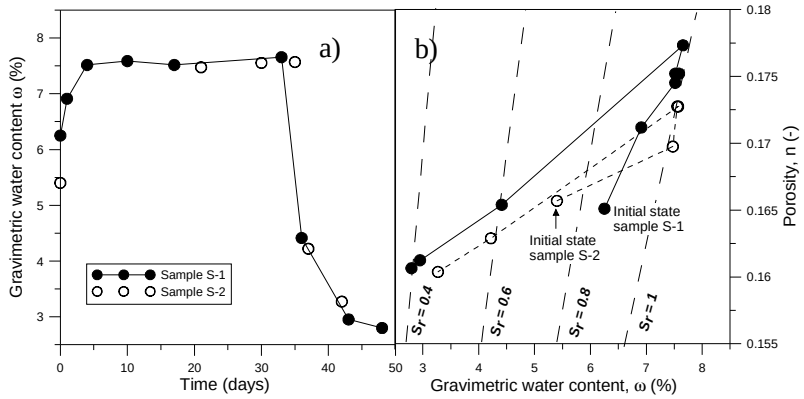

Figure 5. a) Water content versus time; b) volumetric evolution during a wetting-drying cycle

The initial porosity values, Fig. 5b, were about 0.165 for both specimens. However, at the end of wetting stage different porosity values were attained. S-1 reached a porosity value of 0.177 and sample S-2, a lower value of 0.172. Sample S-1 was closer to the heater and, presumably, more damaged. During drying a decrease in rock porosity was observed, and both specimens reached 0.160.

4.2 Evolution of Elastic parameters

The solid symbols for S-1 specimen and empty ones for the S-2 specimen in Figure 5a,b represent the equilibrium states where elastic measurements took place.

4.2.1 Vertical measurements

Figures 6 and 7 show the output and input signals for the bender elements tests performed during the hydraulic cycle on samples S-1 and S-2, respectively. Estimated travel time is indicated by a dotted lined on each output trace, thus allowing its variation with wetting and drying paths to be directly observed. Although absolute values are not available, the application of the wetting path shows a relative increase of material attenuation with saturation. The quality of output traces was, however, adequate for arrival time selection. The evolution of the shear wave velocity in vertical direction ($V_{s(vh)}$) with gravimetric water content is shown in Figure 8. In the same figure, the results of the ultrasonic pulse tests for determining the bar wave velocity ($V_{p(v)}$) are reported. The response shows significant differences between specimens S-1 and S-2. Lower initial values for both bar and shear waves were obtained for specimen S-1 (2093 and 1030m/s, respectively) than for specimen S-2

(2795 and 1883m/s). It is worth recalling the sample S-1 was located nearer to the heater (0.2m) than sample S-2 (0.5 m).

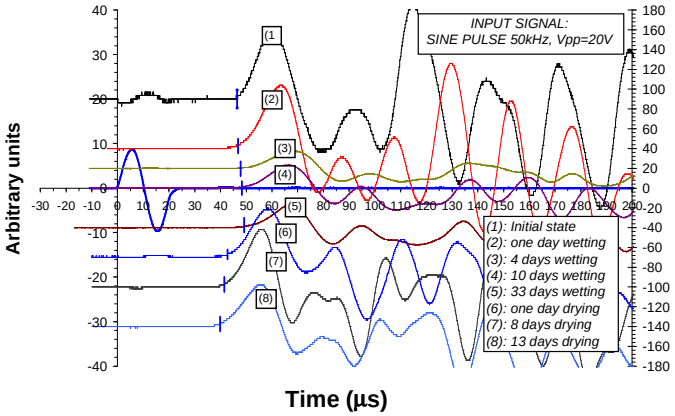

Figure 6. Output traces obtained during bender elements tests for specimen S-1

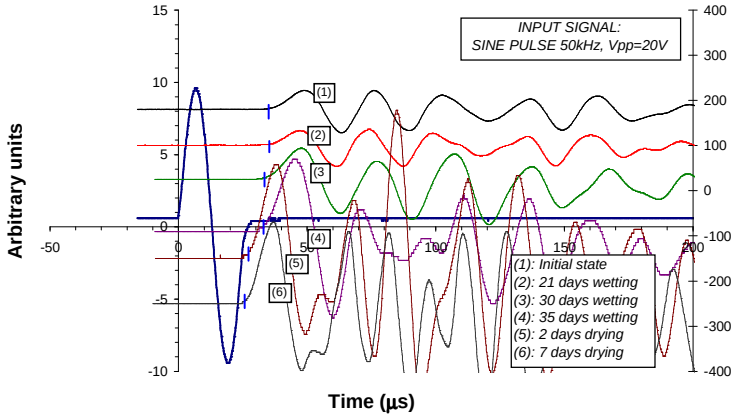

Figure 7. Output traces obtained during bender elements tests for specimen S-2

As wetting proceeds, both compression and shear wave velocities decrease until an equilibrium value is attained at quasi-saturation. The decrease was smaller for sample S-1, which started with a higher initial degree of saturation. The velocity gradients during drying ($dV_{p(v)}/d\omega$ and $dV_{s(vh)}/d\omega$) were evaluated and are also included in Figure 8. It is clear that the stiffening effect of water content change is higher in specimen S-2 than in S-1. This suggests a more intact soil structure in specimen S-2.

4.2.2 Horizontal bender element measurements

Figure 9 shows the output traces obtained by horizontal bender element measurements during the application of the wetting-drying cycle on specimen S-2. A short-circuit in the $V_{s(hv)}$ transducer meant that only the horizontal wave polarized in horizontal direction ($V_{s(hh)}$) was measured. The output traces (Fig. 9) seem affected by electro-magnetic coupling or “cross-talk” effects, thus the determination of the travel time is not straightforward, despite the good reception of the mechanical wave. Thus, the first attempts of horizontal measurements in unconfined conditions were not successful and additional tests are under course to improve this aspect.

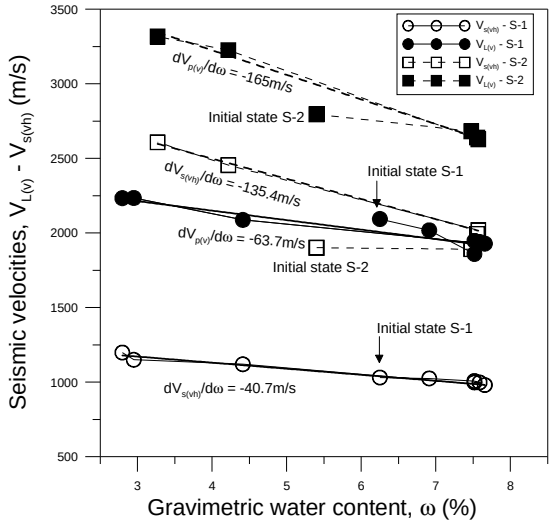

Figure 8. Seismic velocities against gravimetric water content

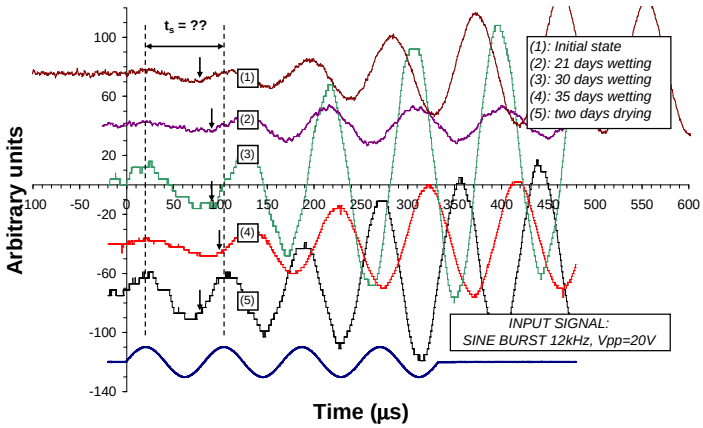

Figure 9. Horizontal bender element traces in Opalinus clay S-2 specimen

5. DISCUSSION

The experimental results presented in Figure 8 show a quasi-linear variation for both bar and shear wave velocities during the application of the hydraulic cycle, and particularly during the drying path. The WRC (Fig. 2) shows also a quasi-linear variation between water content and total suction, s. Elastic wave velocities and total suction might be related using logarithmic regression (Figure 10a). That is

$$V_{L,s(ij)}(s) = V_{L,s(ij)}(s_{(0)}) + \beta * \ln\left(\frac{s}{p_{ref}}\right) \qquad (1)$$

where $V_{L,s(ij)}(s_{(0)})$ is the value for either bar or shear wave velocity at zero total suction (Sr=1), β a material parameter expressed in (m/s) and p_{ref} is a reference pressure and it is equal to 1 (using the same units that suction). For bar velocities, β was 229.9 and 88 for S-2 and S-1, respectively. For shear wave velocities β was 186.8 and 57.8 for samples S-2 and S-1, respectively. The parameter β seems dependent on rock damage. Saturation is the main cause of velocity changes, since porosity changes are relatively

small (Fig 10b).

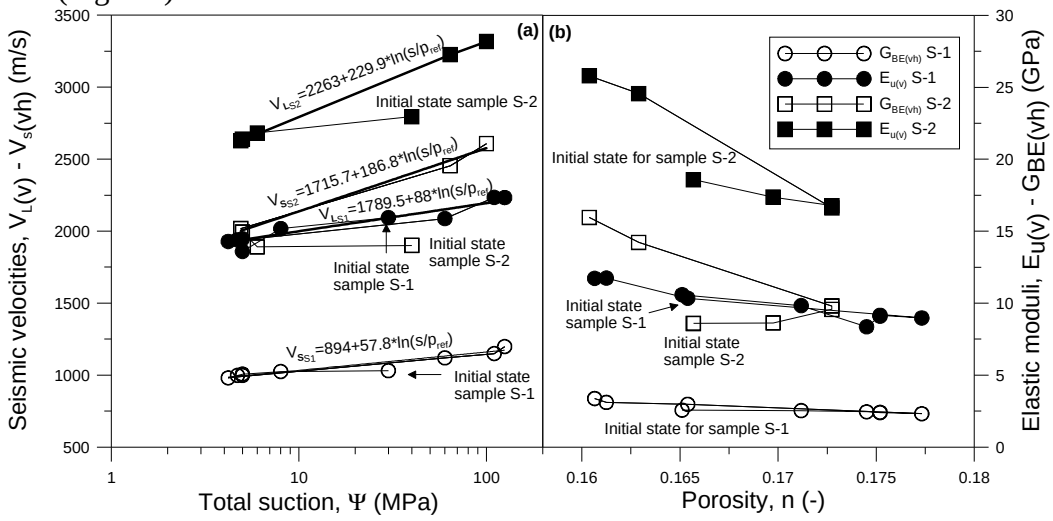

Figure 10:a) Seismic velocities against total suction; b) seismic properties against porosity

ACKNOWLEDGEMENTS

The second author was supported by the EU ALBAN PROGRAMME grant number E04D027285CO. A. Gens, J. Vaunat and B. Garitte facilitated the clay samples

6. REFERENCES

1 Gens A., Vaunat J., Garitte B. & Wileveau Y. 2007. "In situ behaviour of a stiff layered clay subject to thermal loading: observations and interpretation". Géotechnique 57(2).

2 Mayor J.C., Velasco M. & García-Siñeriz J.L. 2007. "Ventilation experiment in the Mont Terri underground laboratory". *Physics and chemistry of the earth, 32, pp. 616-628.*

3 Bock H. 2001."RA experiment. Rock mechanics analyses and synthesis: Data report on rock mechanics", *Technical report 2000-02, Mont Terri project*

4 Pennington, D.S., Nash, D.F.T. & Lings, M.L. 1997. "Anisotropy of G0 shear stiffness in Gault Clay", *Géotechnique, 47, No. 3, 391-398.*

5 Bossart P., Meier P.M., Moeri A., Trick T. & Mayor J.C. 2002. "Geological and hydraulic characterisation of the excavation disturbed zone in Opalinus clay of the Mont Teri Rock Laboratory". *Engineering Geology, vol 66, pp. 19-38.*

6 Muñoz J.J. 2007. "Thermo-hydro-mechanical analysis of soft rock: application to a large scale heating test and large scale ventilation test". *PhD Thesis, Universitat Politècnica de Catalunya, Barcelona.*

7 Decagon Devices, Inc. 2003. WP4 Water Dewpoint Potentiometer. Operator's Manual Version 2.2. Decagon Devices, Inc., Pullman, USA (www.decagon.com).

8 Romero, E.E. 2001. "Controlled suction techniques". *Proc. 4º Simposio Brasileiro de Solos Nao Saturados. Gehling and Schnaid Edits. Porto Alegre, Brasil, pp. 535-542.*

9 Cardoso, R., Romero, E., Lima, A. and Ferrari, A. 2007. "A comparative study of soil suction measurement using two different high-range psychrometers". *Proc. Mechanics of unsaturated soils. Schanz editor.*

10 Shirley D.J. and Hampton L.D. 1978. "Shear-wave measurements in laboratory sediments". *J. Acoustical Soc. Am. 63, n 2, pp. 607-613*

11 Viggiani G. & Atkinson J.H. (1995) Interpretation of bender element test. Géotechnique 45(1), pp. 149-154.

12 Pineda, J.A. 2009 "Swelling and degradation of argillaceous rocks". *PhD Thesis, Universitat Politécnica de Catalunya, Barcelona (in progress)*

13 Pineda, J.A., Arroyo M., Romero E. & Alonso E.E. 2008. "Dynamic tracking of hydraulically claystone degradation". *Proc. 4th Int. Symp. Deformation Characteristics of Geomaterials. Burns, Mayne & Santamarina Eds., pp. 809-816.*